SAGE Publishing

Research Article

Highly Sensitive Detection of Trace Tetracycline in Water Using a Metal-Organic Framework-Enabled Sensor

Jiezeng Chen,[1,2] **Hongying Shu,**[2] **Pingping Niu,**[1,2] **Pinghua Chen** ⓘ**,**[1,2] **and Hualin Jiang** ⓘ[1,2]

[1]*Key Laboratory of Jiangxi Province for Persistent Pollutants Control and Resources Recycle, Nanchang Hangkong University, Nanchang 330063, China*
[2]*Department of Applied Chemistry, College of Environmental and Chemical Engineering, Nanchang Hangkong University, Nanchang 330063, China*

Correspondence should be addressed to Pinghua Chen; cph1979@126.com and Hualin Jiang; hua20022000@126.com

Due to the abuse application of antibiotics in the recent decades, a high level of antibiotics has been let out and remains in our environment. Electrochemical sensing is a useful method to sensitively detect antibiotics, and the key factor for a successful electrochemical sensor is the active electrode materials. In this study, a sensitive electrochemical sensing platform based on a metal-organic framework (MOF) of MIL-53 (Fe) was facilely fabricated. It shows highly selective and sensitive detection performance for trace tetracycline. Differential pulse voltammetry (DPV) was applied to analyze the detection of tetracycline. The linear range of tetracycline detection was 0.0643 μmol/L-1.53 μmol/L, and the limit of detection (LOD) is 0.0260 μmol/L. Furthermore, the MOF-enabled sensor can be effectively used in actual water bodies. The results indicate that the electrochemical sensor is a high potential sensing platform for tetracycline.

1. Introduction

Tetracycline is a typical antibiotic which has been widely used to treat infections caused by Gram-positive and Gram-negative bacterium in both human and animals. Furthermore, it has been also used as growth promoting agents in livestock breeding industry [1]. Because of its low cost and wide-spectrum antibacterial activity, abuse application of tetracycline was common in the past decades. As a result, high tetracycline residue was detected in lots of environmental areas nowadays, including soil, water, and animal productions [2]. Long-term exposure to antibiotics can cause directed toxicity or result in allergies, also boosting the prevalence of antibiotic resistance [3–6]. Tetracycline, as one of the most applied antibiotics, is considered to be carcinogenic, and depressive to bone growth besides the common adverse effects of antibiotics [7]. Tetracycline is a typical emerging contaminant (ECs), which usually refers to those highly concerned environmental substances because of their detecting frequency and potential dangers, but the environmental

management details such as monitor regulations and emission control limits are still in blank [8]. Thereafter, highly sensitive and fast responsive techniques for tetracycline detection are urgently needed, which are important for the governors to formulate the suitable management policies.

Numerous methods have been developed for tetracycline detection. Chromatographic methods are the sensitive methods to detect tetracycline, including high performance liquid chromatography (HPLC) [9], liquid chromatography coupled to mass spectrometry (LCMS) [10], and thin-layer chromatography (TLC) [11]. Nevertheless, some inherent drawbacks, such as time-costing, needing highly professional operators, and luxury devices, significantly limit their wide application. Besides chromatographic methods, some other methods such as capillary electrophoresis (CE) [12] and enzyme-linked immunosorbent assay (ELISA) [13] are also applied to detect tetracycline with good performance. But inherent disadvantages including complicated pretreatments and skilled operation requirement still exist. Therefore, more convenient, rapid, sensitive, and selective techniques are
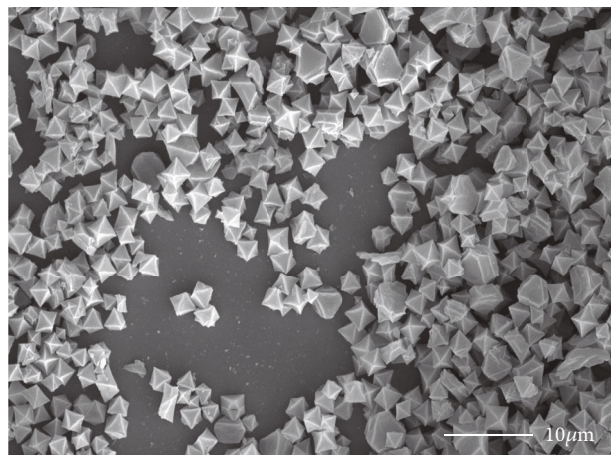
(a)
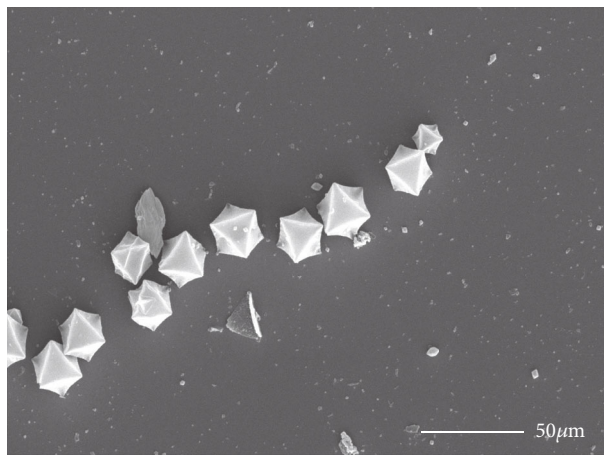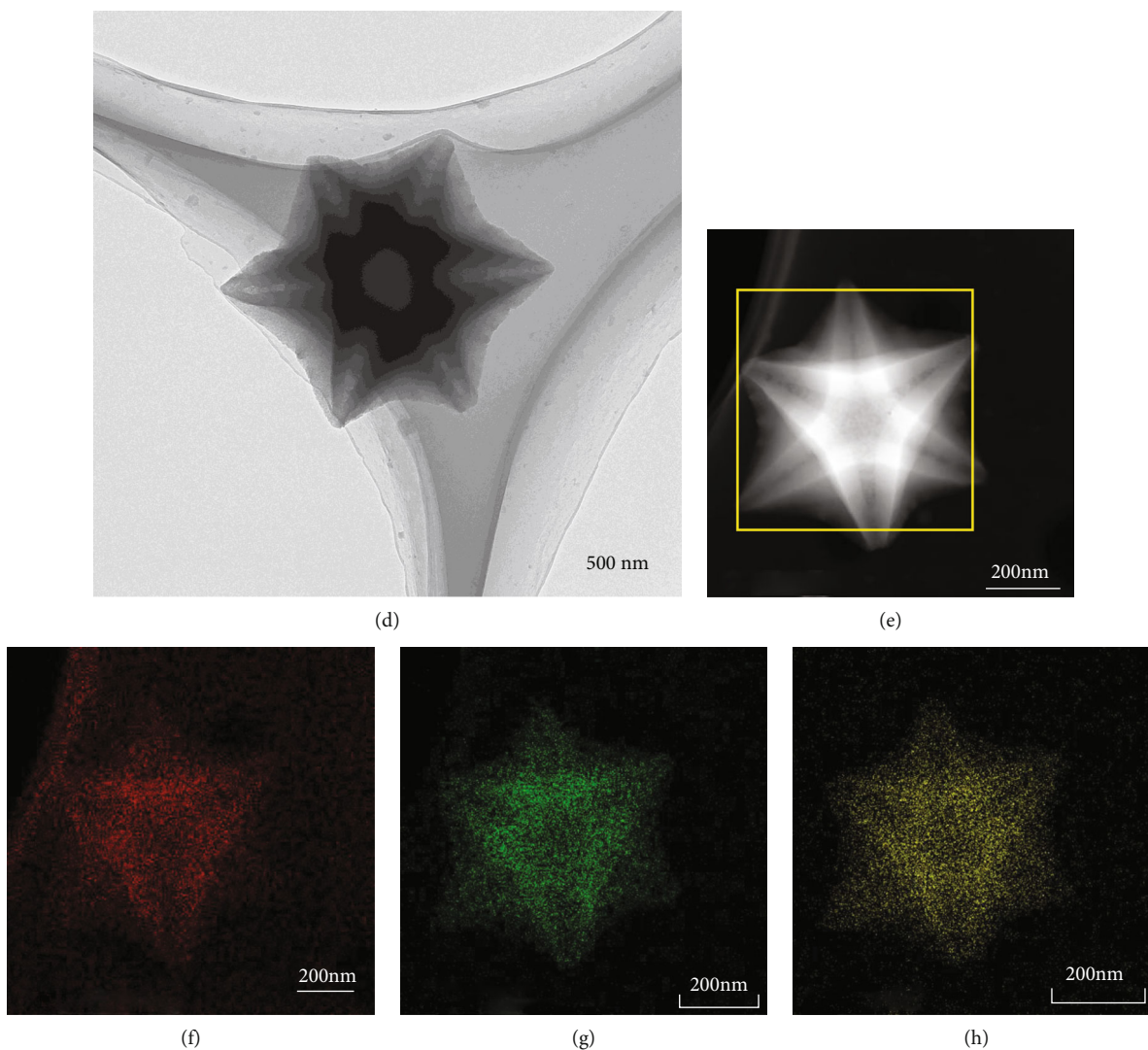

(b)
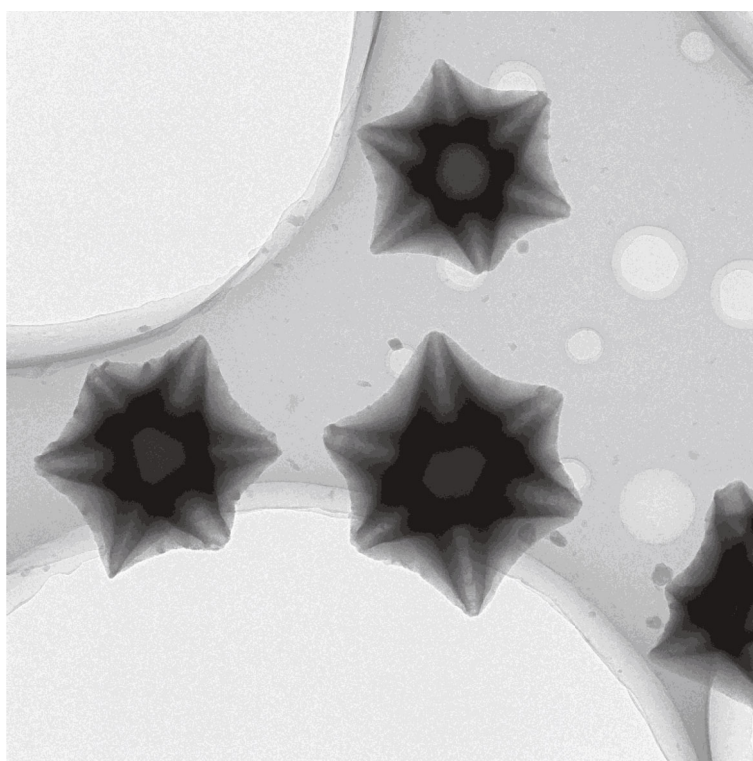
(c)

Figure 1: Continued.

(d)

(e)

(f)

(g)

(h)

FIGURE 1: (a, b) SEM images of MIL-53 (Fe). (c, d) TEM images of MIL-53 (Fe). (e–h) Elemental mapping of MIL-53 (Fe).

highly required in tetracycline detection. Recently, tetracycline detection based on electrochemical sensors rapidly develops owing to their easy operation, high sensitivity, high selectivity, and real-time detection.

Metal-organic frameworks (MOFs), a polymer built by assembling metal ions and lots of organic linkers, has been widely used in catalysis [14], adsorption [15], energy storage [16], sensors [17] and so on, due to their unique advantages of plentiful micropores, large specific surface area, abundant active sites, and varied conformations [18]. Therefore, facile whereas highly performed MOF-enabled electrochemical sensors are highly demanded.

In this study, a simple electrochemical sensing platform based on a Fe containing MOF, MIL-53 (Fe), modified glass carbon electrode (denoted as MIL-53 (Fe)/GCE) was facilely fabricated. The present work demonstrates that MIL-53 (Fe)/GCE shows highly sensitive detection performance for trace tetracycline, indicating its high potential in effective electrochemical sensor application due to the easy fabrication, high sensitivity, and low cost.

2. Materials and Methods

2.1. Materials. N, N-dimethylformamide (DMF), absolute ethanol (CH_3CH_2OH), and ferric chloride hexahydrate ($FeCl_3 \cdot 6H_2O$) were obtained from Sinopharm Chemical Reagent Co., Ltd. (Shanghai, China). p-Phthalic acid ($C_8H_6O_4$, H_2BDC) and tetracycline ($C_{22}H_{24}N_2O_8 \cdot xH_2O$) were bought from Aladdin, China. Other chemicals were all commercial with analytical grade and used directly. Deionized water (DI water) was used through the experiments.

2.2. Preparation of MIL-53 (Fe). 0.68 g (2.5 mmol) $FeCl_3 \cdot 6H_2O$ and 0.42 g (2.5 mmol) p-phthalic acid (H_2BDC) were resolved completely in 54 mL DMF. Then, the mixture was placed into a stainless steel autoclave with Teflon lining to react at 150°C for 15 h. After that, the solid was separated and thoroughly washed. Finally, the solid was dried to obtain the MIL-53 (Fe) powder with light orange color [19].
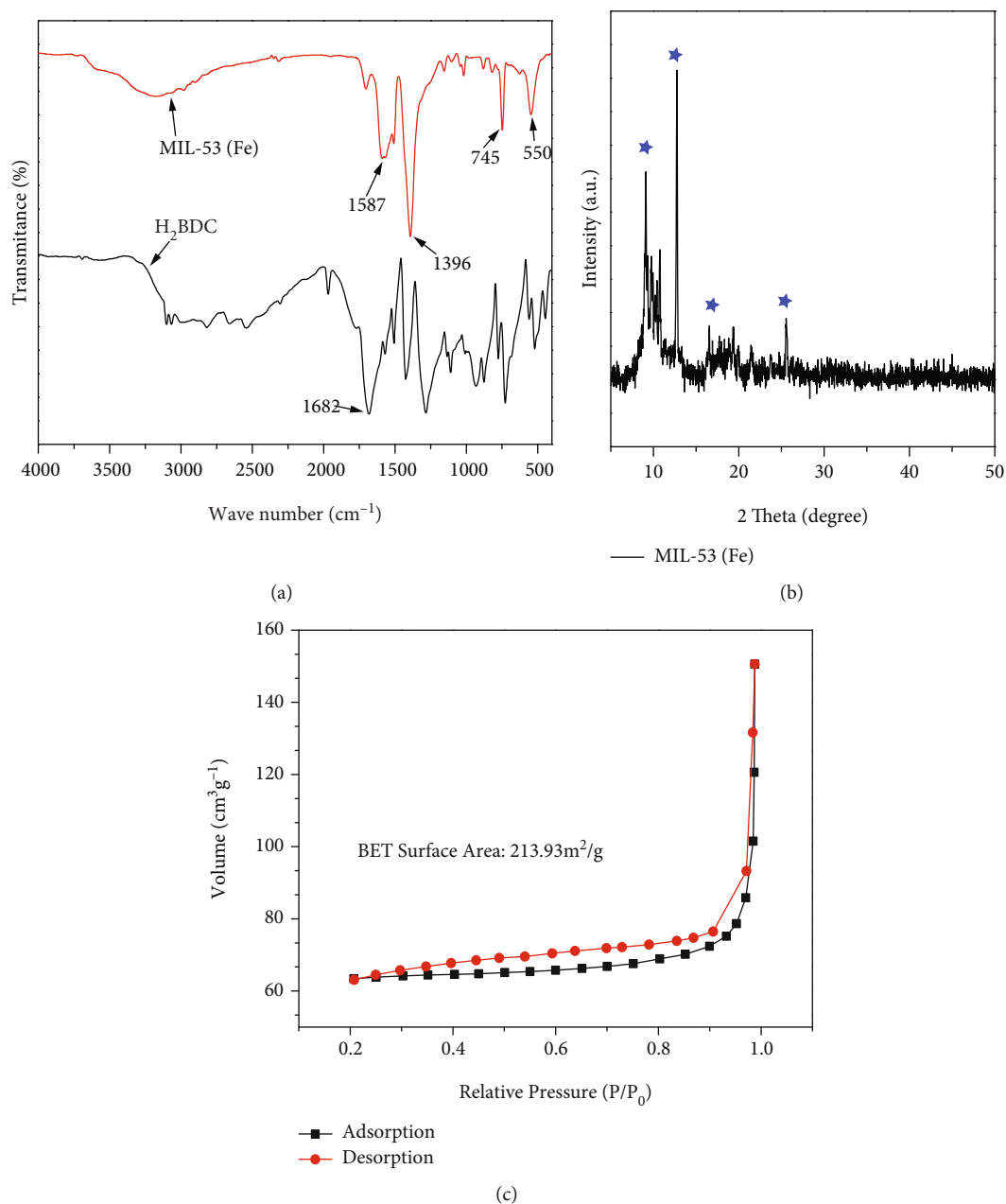
(a)

(b)

(c)

FIGURE 2: (a) FT-IR spectrum of the as-synthesized MIL-53 (Fe) and H$_2$BDC. (b) XRD spectra of MIL-53 (Fe). (c) N$_2$ adsorption-desorption isotherms.

2.3. Preparation of MIL-53 (Fe)/GCE. 5 mg MIL-53 (Fe) was dispersed by ultrasonication in 5.0 mL deionized water to form a suspension (1 mg/mL). The GCE (diameter 3 mm) was polished with alumina powder and then ultrasonically washed with dilute nitric acid ($V_{\text{concentrated nitric acid}} : V_{\text{water}}$ = 1 : 1), ethanol, and DI water sequentially. At last, it was dried at room temperature (RT). 8 μL suspension was dropped on the surface of the polished GCE. After it was dried, 8 μL 0.5% Nafion was applied in drops to the surface to obtain the MIL-53 (Fe) modified GCE, denoted as MIL-53 (Fe)/GCE, and then, it was wired for electrical measurements.

2.4. Characterizations. The morphology of MIL-53 (Fe) was studied by scanning electron microscopy (SEM) (Hitachi-4800, Japan) and transmission electron microscope (TEM) (JEM-2100, Japan). Samples were analyzed by X-ray powder diffractometer (XRD, Rigaku III/B max, Cu Ka). Fourier transform infrared spectroscopy (FT-IR) analyses were recorded on a Nicolet 380 (USA) instrument. Brunauer-Emmett-Teller (BET, TriStar II 3020, USA) was analyzed by the N$_2$ adsorption-desorption isotherm.

2.5. Electrochemical Experiments. All the experiments were conducted in a standard three-electrode system by an

electrochemical workstation (CHI660E). Platinum plate electrode and Ag/AgCl (saturated KCl) were employed as a counter electrode and a reference electrode, respectively, and GCE supported by catalyst was used as a working electrode. All subsequent experiments were carried out under the condition of constant temperature at 25°C. Before the experiment, nitrogen was used to purge the electrolyte for degassing.

Differential pulse voltammetry (DPV) and cyclic voltammetry (CV) were tested by adding certain amount of tetracycline in 1 M H_2SO_4. The scanning rate of CV is 100 mV/s, and the voltage range is -0.7 ~ 1.2 V. DPV was applied with voltage range of -0.8 ~ 1.5 V, pulse width of 50 ms, and pulse amplitude of 50 mV.

3. Results and Discussion

3.1. Characterizations of MIL-53 (Fe). The SEM and TEM images of the as-prepared MIL-53 (Fe) are present in Figure 1. As one can see in SEM images (Figures 1(a) and 1(b)), the sample shows a typical octahedral structure, which was further confirmed by the TEM images (Figures 1(c) and 1(d)). Elemental mapping study indicates that C, O, and Fe all exist and uniformly distribute in the sample (Figures 1(e)–1(h)). These observations are consistent with the previous reports of MIL-53(Fe) [20, 21], suggesting the successful synthesis of MIL-53 (Fe).

MIL-53 (Fe) and the ligand p-phthalic acid (H_2BDC) were investigated by FT-IR spectroscopy, and the results are indicated in Figure 2(a). One can see that MIL-53 (Fe) clearly shows distinct peaks at 1587, 1396, 745, and 550 cm^{-1}. The strong adsorption band appearing at 1396 cm^{-1} is ascribed to the symmetric vibrations of the -COOH group, confirming the presence of carboxylate linkages in the framework of MIL-53 (Fe) [22]. The peak at 745 cm^{-1} is due to the bending vibration of the C-H bond from the benzene ring [19, 23]. Furthermore, the band at 550 cm^{-1} is related to the tensile trembling of the Fe-O bond [24], which indicates the formation of Fe-oxo cluster linking the metal and the carboxyl group. H_2BDC shows a clear characteristic band of carboxyl group asymmetric vibrations at 1682 cm^{-1}. It is noted that this band in MIL-53 (Fe) shifts to 1587 cm^{-1}, indicating the carboxyl group of H_2BDC coordinated with the metal center and formed the complex of MIL-53 (Fe) [25]. The FT-IR analysis indicate that MIL-53 (Fe) is successfully synthesized.

The structure of MIL-53 (Fe) was studied by XRD spectra. As shown in Figure 2(b), the spectra exhibits strong adsorption bands at 9.17°, 12.7°, 17.6°, and 25.5°, which are consistent with the characteristic XRD spectra of MIL-53 (Fe) [21]. This result confirms the successful preparation of MIL-53(Fe).

In order to study the surface area and pore diameter of the as-synthetic MIL-53(Fe), the material were subjected to BET analysis. As shown in Figure 2(c), the N_2 adsorption-desorption isotherms shows a typical H3 type hysteresis ring, which indicates the existence of mesopores formed by accumulation. The BET special surface area of MIL-53 (Fe) is calculated to be 213.93 m^2/g. The high BET special area
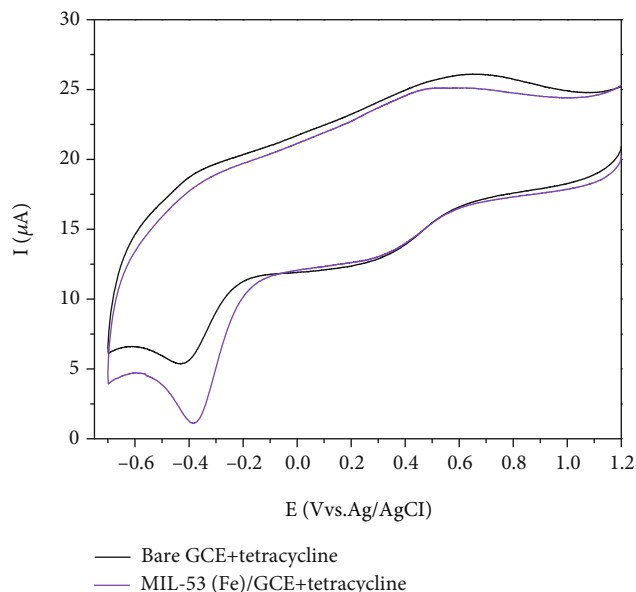

FIGURE 3: CVs of bare GCE and MIL-53 (Fe)/GCE in 1 M H_2SO_4 with 1.278 μmol/L tetracycline, respectively.

and mesopores can increase the molecular interaction between the analyte and the active electrode material, promoting the sensing performance [26–29].

3.2. Electrochemical Characterization of MIL-53 (Fe). The electrochemical behaviors of tetracycline over bare GCE and MIL-53 (Fe)/GCE were investigated in 1 M H_2SO_4 via CV. It can be seen in Figure 3 that the reduction peak in the range of -0.35 to -0.55 V is sensitive, so it is measured as a response signal to compare the difference between the samples. It can be found that the bare GCE shows a little electrochemical response to tetracycline. As GCE was modified with MIL-53 (Fe), its response to tetracycline was significantly improved, which indicates the high electrochemical activity toward tetracycline of MIL-53 (Fe).

3.3. The Effect of pH. The electrochemical responses of the sensor toward tetracycline in different pH conditions were investigated by CV, and the pH was adjusted by H_2SO_4 solution. The experiment was carried out under the following conditions: constant temperature (25°C), tetracycline concentration of 0.641 μmol/L, pH range of 0 to 2.6, voltage range of -0.7 V ~ 1.2 V, and scanning rate of 100 mV/s. As indicated in Figure 4(a), the reduction peak potential (E_p) in the range of -0.35 to -0.55 V is sensitive; therefore, it is measured as a response signal. The reduction peak potential (E_p) and the related peak current (I_p) were plotted with pH values of the supporting electrolyte solution. As one can see in Figure 4(b), when the pH value rises from 0 to 2.6, the peak potential of the cathode changes negatively and is inversely proportional to pH, indicating that protons are directly related to electrochemical reactions [30]. The linear relationship between peak potential (E) and pH over MIL-53 (Fe)/GCE towards tetracycline can be expressed as follows: $E = -0.05013\text{pH} - 0.3837$ ($R^2 = 0.94942$). It can be found that the slope of the linear relationship is close to the
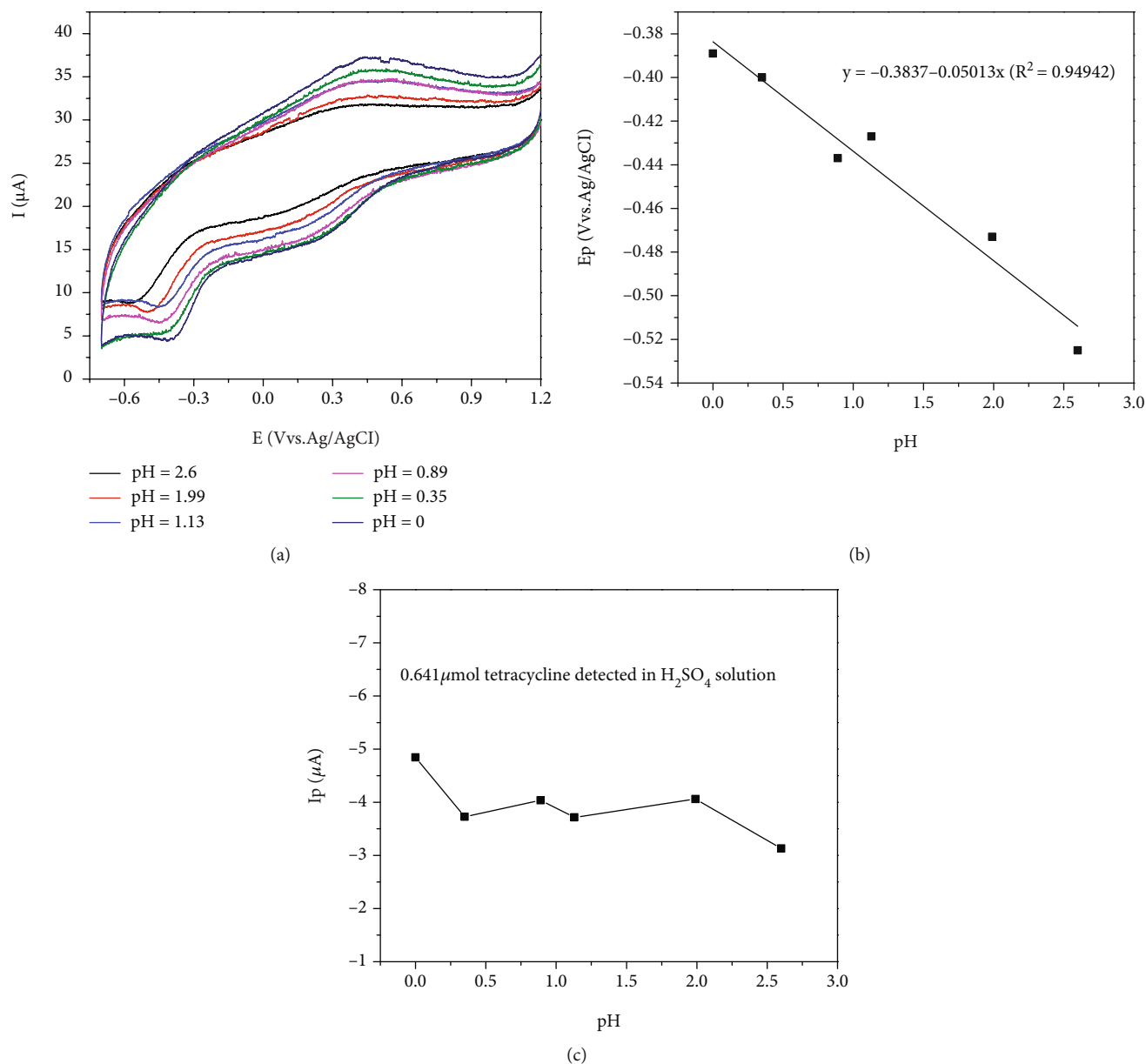
(a)

(b)

(c)

Figure 4: (a) CVs of 0.641 μM tetracycline over MIL-53 (Fe)/GCE in H_2SO_4 solution with different pH values (0-2.6). (b) The dependence of E_p with pH. (c) The dependence of I_p with pH.

theoretical value of 0.059 V/pH (according to the Nernst equation $E = E_0 - (0.059/n) \times pH$) [31], indicating that the detection of tetracycline by MIL-53 (Fe) is an electrochemical reaction that the same amount of proton and electron is involved [30]. As one can see in Figure 4(c), when the pH value is 0, the I_p value is the largest. When the pH rises from 0 to about 0.25, the value of I_p significantly decreases. When the pH changes from 0.25 to 2, the I_p changes a little but relatively stable as compared with the behaviors in other pH ranges, indicating pH does not have much effect on I_p in this range. When the pH is higher than 2.0, the value of I_p dramatically decreases as the pH rises. This result indicates that pH = 0 can be determined as the optimum pH condition, because the highest I_p value is obtained.

3.4. Detecting Range and Limit of MIL-53 (Fe)/GCE.
The detection of tetracycline over MIL-53 (Fe)/GCE was measured by differential pulse voltammetry (DPV) (Figure 5(a)). A certain amount of tetracycline was added in 1 M H_2SO_4 solution, and the DPV was carried out. The concentration of tetracycline and the related peak current (I_p) in DPV at ~0.25 V (I_p) are linearly related over two different continuous concentration ranges (Figure 5(b)). The relevant regression equation is as follows:

0.0643 μmol/L-0.769 μmol/L:

$$Ip\,(\mu A) = -1.3453 * C\left(\frac{\mu mol}{L}\right) - 2.8646\,(R^2 = 9616). \quad (1)$$
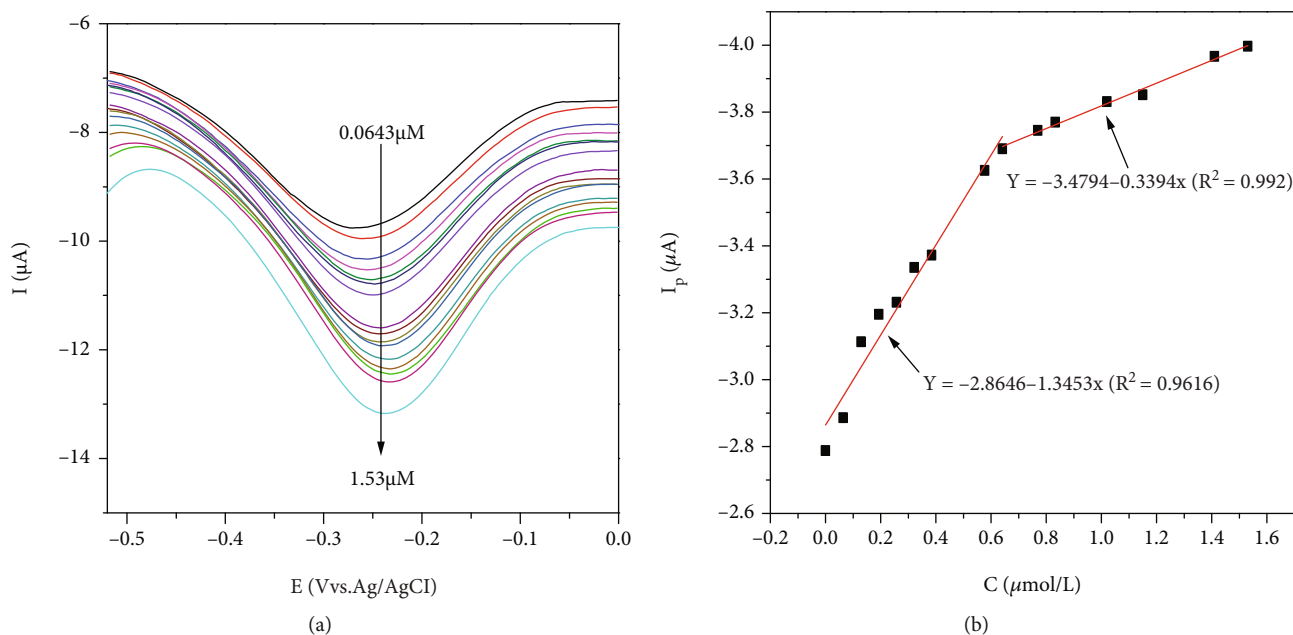
FIGURE 5: (a) DPV of tetracycline with different concentrations in 1 M H_2SO_4 over MIL-53 (Fe)/GCE. (b) The linear dependence of I_p with tetracycline concentration.

TABLE 1: Summary of the tetracycline detecting performance between different sensors.

Sensor types	Detection techniques	Signal transducer or active electrode materials	Linear range (μM)	Detection limit (μM)	References
Optical sensor type	Colorimetric	AuNPs	0.95-29.25	0.38	[33]
		TMB	0.01-1	0.045	[34]
	Fluorescence	MIP-APS-QDs	0.12-0.37	0.54	[35]
		MIP-MAA-QDs	0.10-0.37	0.50	[36]
	SPR	AgNPs	112.5-11250	29.25	[37]
Electrochemical sensor type	DPV	Fe/Zn-MMT/GCE	0.30–52	0.10	[1]
		MIOPPy-AuNP/SPCE	1-20	0.65	[37]
		MWCNTs/GCE	0.01-10	0.005	[38]
		PtNPs/C/GCE	9.99–44.01	4.28	[39]
	CV	UV-DNA/GCE	0.3-90	0.27	[40]
		MIP/MWCNTs-AuNPs/GCE	0.225-90	0.09	[41]
	DPV	MIL-53(Fe)/GCE	0.0643-1.53	0.026	This work

SPR: surface plasmon resonance; DPV: differential pulse voltammetry; CV: cyclic voltammetry; AuNPs: Au nanoparticles; TMB: 3,3′,5,5′-tetramethylbenzidine; MIP-APS-QDs: molecularly imprinting polymer-3-mercapto-propyltriethoxysilane-CdTe quantum dots; MIP-MAA-QDs: molecmolecularly imprinting polymer-methacrylic acid-CdTe quantum dots; AgNPs: Ag nanoparticles; Fe/Zn-MMT/GCE: iron/zinc cation–exchanged montmorillonite catalyst on glassy carbon electrode; MIOPPy-AuNP/SPCE: screen-printed carbon electrodes modified with molecularly imprinted overoxidized polypyrrole and gold nanoparticles; MWCNTs/GCE: multiwalled carbon nanotubes, modified glass carbon electrode; PtNPs/C/GCE: platinum nanoparticles supported on carbon-coated glassy carbon electrode; UV-DNA/GCE: UV irradiated DNA film modified glassy carbon electrode; MIP/MWCNTs-AuNPs/GCE: molecularly imprinting polymer and gold nanoparticles modified multiwalled carbon nanotubes, modified glass carbon electrode.

0.769 μmol/L-1.53 μmol/L:

$$Ip\,(\mu A) = -0.3394 * C\left(\frac{\mu mol}{L}\right) - 3.4794\,\left(R^2 = 0.9920\right).$$

(2)

The limit of detection (LOD) is calculated according to the IUPAC criterion (based on 3 times the signal-to-noise ratio, Equation (3)) [32].
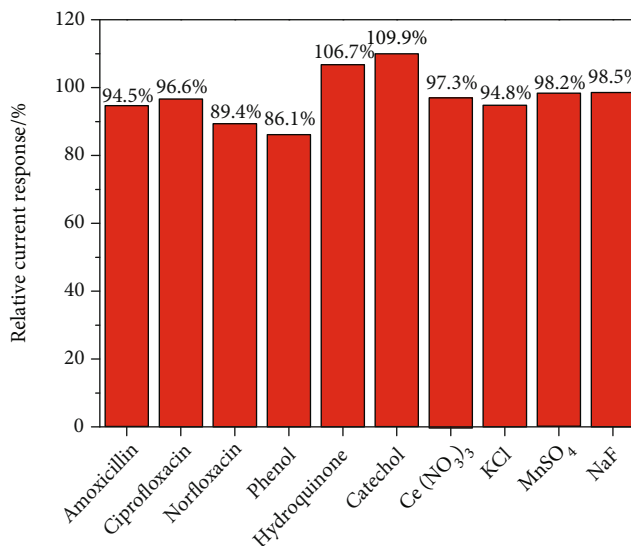
$$LOD = \frac{3\sigma}{k},$$

(3)

FIGURE 6: Amperometric response of MIL-53 (Fe)/GCE to tetracycline (1.278 μmol/L) coexistent with different interfering substances (other antibiotics interferences with 10 times concentration (12.78 μmol/L): amoxicillin, ciprofloxacin, and norfloxacin. Typical organic interferences with 100 times concentration (127.8 μmol/L): phenol, hydroquinone, and catechol. Typical inorganic interferences with 100 times concentration (127.8 μmol/L): Ce^{3+}, NO^{3-}, K^+, Cl^-, Mn^{2+}, Na^+, and F^-). It was pair system that one interference coexistent with tetracycline in one test, and the DPV responses of the sensor to tetracycline were recorded. Other conditions were the same as described elsewhere. The DPV response of the sensor to bare tetracycline was set as the value of 100%.

where σ is the standard deviation of a blank ($n = 20$) and k is the slope of the calibration curve. Therefore, the limit of detection is estimated to be 0.0260 μmol/L.

Because tetracycline is one of the ECs, there is no official permitted limitation of tetracycline in water at present. It is no other than comparison of detecting performance of MIL-53 (Fe)/GCE and other tetracycline sensors can be used to evaluate the detecting efficiency of MIL-53 (Fe)/GCE. For this purpose, the parameters of detection techniques, linear range, and limit of detection of MIL-53 (Fe)/GCE were compared to other reported tetracycline sensors. As one can see in Table 1, the performance of MIL-53 (Fe)/GCE is comparable with those of others, even higher in some aspects (especially the detection limit). The comparison indicate that MIL-53 (Fe)/GCE is an effective sensing platform, which can sufficiently meet the requirement of tetracycline detection application.

3.5. Selective Study. To evaluate the selectivity of the electrochemical sensor for tetracycline, the interfering substances (with significantly high concentrations than tetracycline) that may occur during the detection of tetracycline were studied. As shown in Figure 6, typical organic interferences such as phenol, hydroquinone, and catechol have a little effect on the detection of tetracycline. When inorganic ions such as Ce^{3+}, NO^{3-}, K^+, Cl^-, Mn^{2+}, Na^+, and F^- was added, there is no significant change in the amperometric response of tetracycline. When other antibiotics (such as amoxicillin, ciprofloxacin, and norfloxacin) are present in the solution of tetracycline, there is almost no effect on the detection of tetracycline. The above results indicate

that MIL-53 (Fe)/GCE has a high selectivity to detect tetracycline.

3.6. Reproducibility and Stability of Modified Electrodes. For the purpose of characterizing the repeatability of the sensor for tetracycline detection, seven different glassy carbon electrodes were applied to prepare seven different MIL-53 (Fe)/GCEs, and their tetracycline detection performance were measured. After 7 parallel measurements, the relative standard deviation (RSD) was obtained as 7.3% (Figure 7(a)), showing that the sensor has a high repeatability to detect tetracycline. For the purpose of investigating the stability of the sensor, 100 cycles of voltammetric scanning were performed. As indicated in Figure 7(b), after 100 CV cycles, there is no significant change in the reduction peak current, showing that the sensor has a high stability. The periodic stability of the sensor was evaluated, too. 3 weeks later after MIL-53 (Fe)/GCE was placed in air at RT, the sensor was employed to measure tetracycline via DPV again (detection conditions are the same as above). The results showed that an initial I_p value of more than 96% was retained (Figure 7(c)), showing the high period stability of the sensor.

3.7. Application in Actual Water. Natural water samples including tap water and river water were used to evaluate the practical application of MIL-53(Fe)/GCE. Tetracycline (with three concentrations of 0.321 μM, 0.641 μM, and 1.278 μM) were spiked into the above actual water samples due to no tetracycline being detected in the original samples. The recovery results are shown in Table 2. One can
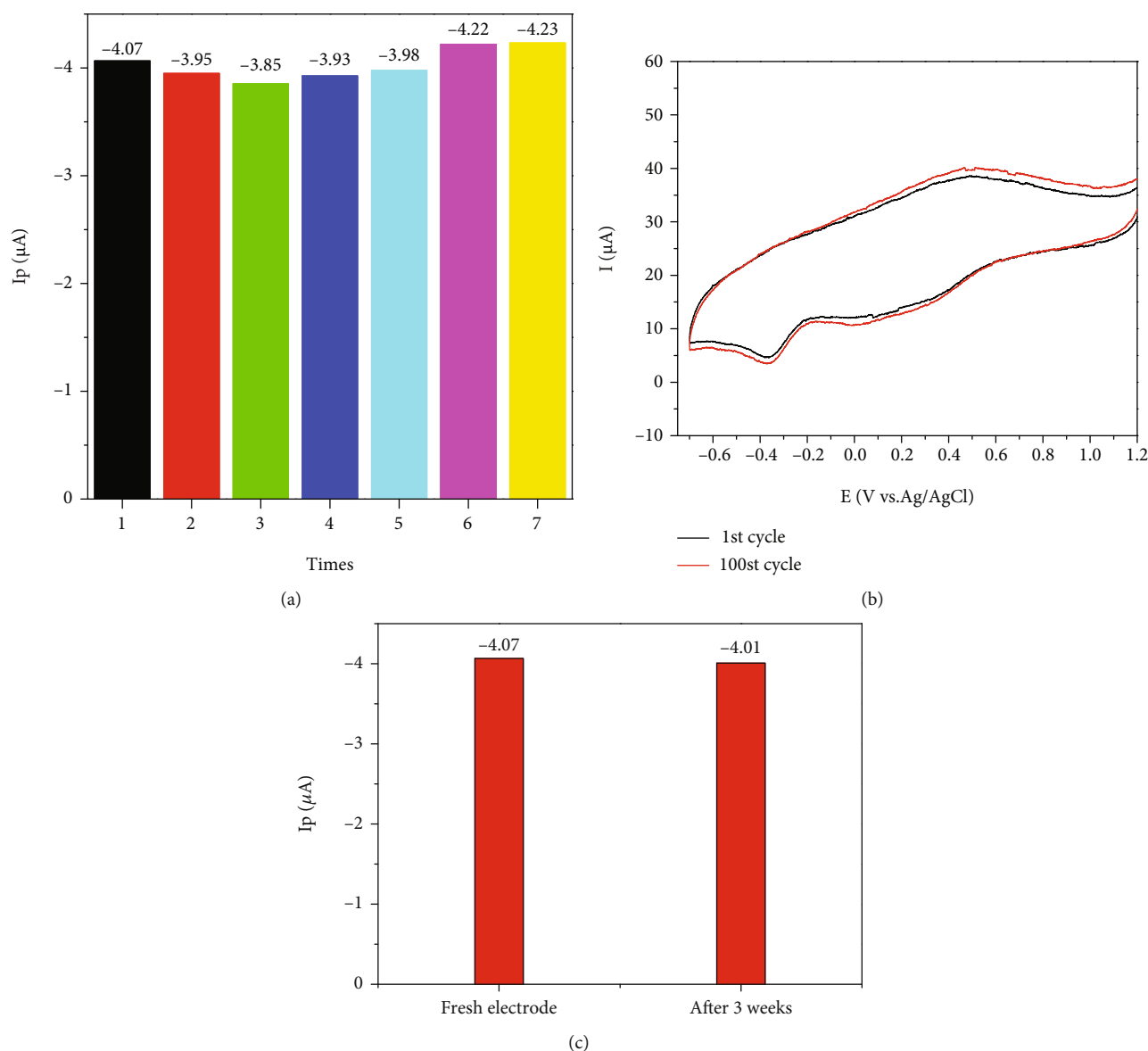
(a)

(b)

(c)

FIGURE 7: (a) The peak current values of DPVs of 1.278 μM tetracycline in 1 M H_2SO_4 over 7 different MIL-53 (Fe)/GCEs. (b) The CVs of 0.641 μM tetracycline in 1 M H_2SO_4 detected by MIL-53 (Fe)/GCE in the first and 100th cycle. (c) The I_p values of DPVs of 1.278 μM tetracycline in 1 M H_2SO_4 over MIL-53 (Fe)/GCE and that after 3 weeks.

TABLE 2: Detection of tetracycline in tap water and river water.

Sample	Added tetracycline (M)	Found tetracycline (M)	Recovery (%)
Tap water	3.21×10^{-7}	3.61×10^{-7}	112.46
Tap water	6.41×10^{-7}	5.97×10^{-7}	93.14
Tap water	1.278×10^{-6}	1.06×10^{-6}	82.94
River water	3.21×10^{-7}	3.70×10^{-7}	115.26
River water	6.41×10^{-7}	6.95×10^{-7}	108.42
River water	1.278×10^{-6}	1.35×10^{-6}	105.63

see that the sensor has relative high recovery rates in actual water.

4. Conclusion

An electrochemical polymer sensor of tetracycline based on MIL-53 (Fe) was successfully developed in this work. It shows high tetracycline sensing performance in concentration range of 0.0643 μmol/L-0.769 μmol/L and 0.769-1.53 μmol/L, and the LOD can reach 0.0260 μmol/L. The sensor exhibits high reproducibility, anti-interference ability, and stability. Moreover, it can be efficiently used in actual water bodies. The polymer sensor can be facilely prepared and applied with high sensitivity. It has a high potential in practical application of trace tetracycline detection.

Data Availability

The data used to support the findings of this study are included within the article.

Conflicts of Interest

The authors declare no conflicts of interest.

Acknowledgments

References

[1] T. Gan, Z. X. Shi, J. Y. Sun, and Y. M. Liu, "Simple and novel electrochemical sensor for the determination of tetracycline based on iron/zinc cations-exchanged montmorillonite catalyst," *Talanta*, vol. 121, pp. 187–193, 2014.

[2] A. Benvidi, S. Yazdanparast, M. Rezaeinasab, M. D. Tezerjani, and S. Abbasi, "Designing and fabrication of a novel sensitive electrochemical aptasensor based on poly (L-glutamic acid)/MWCNTs modified glassy carbon electrode for determination of tetracycline," *Journal of Electroanalytical Chemistry*, vol. 808, pp. 311–320, 2018.

[3] D. Song, X. Jiang, Y. Li et al., "Metal–organic frameworks-derived MnO_2/Mn_3O_4 microcuboids with hierarchically ordered nanosheets and Ti_3C_2 MXene/Au NPs composites for electrochemical pesticide detection," *Journal of Hazardous Materials*, vol. 373, pp. 367–376, 2019.

[4] C. Fan, X. Zhang, N. Li et al., "Zn-MOFs based luminescent sensors for selective and highly sensitive detection of Fe^{3+} and tetracycline antibiotic," *Journal of Pharmaceutical and Biomedical Analysis*, vol. 188, 2020.

[5] J. Wenliang, L. Liu, X. Jin et al., "Co-inoculation effect of plant-growth-promoting rhizobacteria and rhizobium on EDDS assisted phytoremediation of cu contaminated soils," *Chemosphere*, vol. 254, article 126724, 2020.

[6] C. Zhang, J. Wang, G. Liu, Z. Song, and L. Fang, "Impact of soil leachate on microbial biomass and diversity affected by plant diversity," *Plant and Soil*, vol. 439, pp. 505–523, 2019.

[7] C. M. Calixto, P. Cervini, and É. T. Cavalheiro, "Determination of tetracycline in environmental water samples at a graphite-polyurethane composite electrode," *Journal of the Brazilian Chemical Society*, vol. 23, pp. 938–943, 2012.

[8] M. Petrović, S. Gonzalez, and D. Barceló, "Analysis and removal of emerging contaminants in wastewater and drinking water," *TrAC Trends in Analytical Chemistry*, vol. 22, pp. 685–696, 2003.

[9] J. Li, L. Chen, X. Wang et al., "Determination of tetracyclines residues in honey by on-line solid-phase extraction high-performance liquid chromatography," *Talanta*, vol. 75, pp. 1245–1252, 2008.

[10] Q. Zhou, Y. Y. Zhang, N. Wang, L. H. Zhu, and H. Q. Tang, "Analysis of tetracyclines in chicken tissues and dung using LC–MS coupled with ultrasound-assisted enzymatic hydrolysis," *Food Control*, vol. 46, pp. 324–331, 2014.

[11] W. Naidong, S. Hua, E. Roets, and J. Hoogmartens, "Assay and purity control of tetracycline, chlortetracycline and oxytetra-cycline in animal feeds and premixes by TLC densitometry with fluorescence detection," *Journal of pharmaceutical and biomedical analysis*, vol. 33, pp. 85–93, 2003.

[12] P. Kowalski, "Capillary electrophoretic method for the simultaneous determination of tetracycline residues in fish samples," *Journal of pharmaceutical and biomedical analysis*, vol. 47, pp. 487–493, 2008.

[13] D. S. Aga, R. Goldfish, and P. Kulshrestha, "Application of ELISA in determining the fate of tetracyclines in land-applied livestock wastes," *The Analyst*, vol. 128, no. 6, pp. 658–662, 2003.

[14] Z. Zhang, Y. Xiao, Y. Lei, J. Tang, and X. Qiao, "Catalytic hydrolysis of β-lactam antibiotics via MOF-derived MgO nanoparticles embedded on nanocast silica," *Science of The Total Environment*, vol. 738, article 139742, 2020.

[15] M. A. Ahsan, V. Jabbari, M. T. Islam et al., "Sustainable synthesis and remarkable adsorption capacity of MOF/graphene oxide and MOF/CNT based hybrid nanocomposites for the removal of bisphenol A from water," *Science of the Total Environment*, vol. 673, pp. 306–317, 2019.

[16] D. P. Dubal, K. Jayaramulu, J. Sunil et al., "Metal–organic framework (MOF) derived electrodes with robust and fast lithium storage for Li-ion hybrid capacitors," *Advanced Functional Materials*, vol. 29, no. 19, 2019.

[17] Y. Cao, L. Wang, C. Shen, C. Wang, X. Hu, and G. Wang, "An electrochemical sensor on the hierarchically porous Cu-BTC MOF platform for glyphosate determination," *Sensors and Actuators B: Chemical*, vol. 283, pp. 487–494, 2019.

[18] Y. Wan, J. Wan, Y. Ma, Y. Wang, and T. Luo, "Sustainable synthesis of modulated Fe-MOFs with enhanced catalyst performance for persulfate to degrade organic pollutants," *Science of The Total Environment*, vol. 701, 2020.

[19] P. Horcajada, C. Serre, G. Maurin et al., "Flexible porous metal-organic frameworks for a controlled drug delivery," *Journal of the American Chemical Society*, vol. 130, no. 21, pp. 6774–6780, 2008.

[20] X. Feng, H. Chen, and F. Jiang, "In-situ ethylenediamine-assisted synthesis of a magnetic iron-based metal-organic framework MIL-53 (Fe) for visible light photocatalysis," *Journal of Colloid and Interface Science*, vol. 494, pp. 32–37, 2017.

[21] C. H. Zhang, W. Q. Hu, H. Jiang et al., "Electrochemical performance of MIL-53(Fe)@RGO as an Organic Anode Material for Li-ion Batteries," *Electrochimica Acta*, vol. 246, pp. 528–535, 2017.

[22] C. H. Zhang, L. H. Ai, and J. Jiang, "Graphene hybridized photoactive iron terephthalate with enhanced photocatalytic activity for the degradation of rhodamine B under visible light," *Industrial and Engineering Chemistry Research*, vol. 54, no. 1, pp. 153–163, 2015.

[23] A. Banerjee, R. Gokhale, S. Bhatnagar et al., "MOF derived porous carbon–Fe_3O_4 nanocomposite as a high performance, recyclable environmental superadsorbent," *Journal of Materials Chemistry*, vol. 22, no. 37, pp. 19694–19699, 2012.

[24] C. Gong, D. Chen, X. Jiao, and Q. L. Wang, "Continuous hollow α-Fe_2O_3 and α-Fe fibers prepared by the sol–gel method," *Journal of Materials Chemistry*, vol. 12, no. 6, pp. 1844–1847, 2002.

[25] R. Liang, F. Jing, L. Shen, N. Qin, and L. Wu, "MIL-53(Fe) as a highly efficient bifunctional photocatalyst for the simultaneous reduction of Cr(VI) and oxidation of dyes," *Journal of Hazardous Materials*, vol. 287, pp. 364–372, 2015.

[26] M. Ghanbarian, S. Zeinali, and A. Mostafavi, "A novel MIL-53(Cr-Fe)/Ag/CNT nanocomposite based resistive sensor for sensing of volatile organic compounds," *Sensors and Actuators B: Chemical*, vol. 267, pp. 381–391, 2018.

[27] C. Wan, W. Wu, C. Wu, J. Xu, and L. Guan, "A layered porous ZrO_2/RGO composite as sulfur host for lithium-sulfur batteries," *RSC Advances*, vol. 5, no. 7, pp. 5102–5106, 2015.

[28] X. Liang, X. Chen, Z. Xiang et al., "Design and synthesis of surface-controlled CuO_x/rGO nanocomposites with unusually high efficiency in catalytic conversion of organic reactants in the presence of $NaBH_4$," *Applied Surface Science*, vol. 459, pp. 716–722, 2018.

[29] S. Navazani, A. Shokuhfar, M. Hassanisadi, A. di Carlo, N. Yaghoobi Nia, and A. Agresti, "A PdPt decorated SnO_2-rGO nanohybrid for high- performance resistive sensing of methane," *Journal of the Taiwan Institute of Chemical Engineers*, vol. 95, pp. 438–451, 2019.

[30] A. E. Vilian, S. R. Choe, K. Giribabu et al., "Pd nanospheres decorated reduced graphene oxide with multi-functions: highly efficient catalytic reduction and ultrasensitive sensing of hazardous 4-nitrophenol pollutant," *Journal of Hazardous Materials*, vol. 333, pp. 54–62, 2017.

[31] J. Zhang, Q. Mei, Y. Ding, K. Guo, X. Yang, and J. Zhao, "Ordered mesoporous $NiCo_2O_4$ nanospheres as a novel electrocatalyst platform for 1-Naphthol and 2-Naphthol individual sensing application," *ACS applied materials & interfaces*, vol. 9, pp. 29771–29781, 2017.

[32] C. Li, X. Zhang, S. Wen et al., "Interface engineering of zeolite imidazolate framework–8 on two-dimensional Al–metal–organic framework nanoplates enhancing performance for simultaneous capture and sensing tetracyclines," *Journal of Hazardous Materials*, vol. 395, 2020.

[33] L. Shen, J. Chen, N. Li, P. L. He, and Z. Li, "Rapid colorimetric sensing of tetracycline antibiotics with in situ growth of gold nanoparticles," *Analytica Chimica Acta*, vol. 839, pp. 83–90, 2014.

[34] Y. L. Wang, Y. J. Sun, H. C. Dai et al., "A colorimetric biosensor using Fe_3O_4 nanoparticles for highly sensitive and selective detection of tetracyclines," *Sensors and Actuators B: Chemical*, vol. 236, pp. 621–626, 2016.

[35] M. R. Chao, C. W. Hu, and J. L. Chen, "Comparative syntheses of tetracycline-imprinted polymeric silicate and acrylate on CdTe quantum dots as fluorescent sensors," *Biosensors & Bioelectronics*, vol. 61, pp. 471–477, 2014.

[36] M. Amjadi, J. L. Manzoori, and F. Pakpoor, "Photometric determination of tetracycline based on surface plasmon resonance of silver nanoparticles," *Journal of Analytical Chemistry*, vol. 71, no. 3, pp. 253–258, 2016.

[37] L. Devkota, L. T. Nguyen, T. T. Vu, and B. Piro, "Electrochemical determination of tetracycline using AuNP-coated molecularly imprinted overoxidized polypyrrole sensing interface," *Electrochimica Acta*, vol. 270, pp. 535–542, 2018.

[38] L. Zhou, D. J. Li, L. Gai, J. P. Wang, and Y. B. Li, "Electrochemical aptasensor for the detection of tetracycline with multi-walled carbon nanotubes amplification," *Sensors and Actuators B: Chemical*, vol. 162, no. 1, pp. 201–208, 2012.

[39] R. T. Kushikawa, M. R. Silva, A. C. Angelo, and M. F. S. Teixeira, "Construction of an electrochemical sensing platform based on platinum nanoparticles supported on carbon for tetracycline determination," *Sensors and Actuators B: Chemical*, vol. 228, pp. 207–213, 2016.

[40] M. B. Gholivand and H. Khani, "Determination of tetracycline at a UV-irradiated DNA film modified glassy carbon electrode," *Electroanalysis*, vol. 25, no. 2, pp. 461–467, 2013.

[41] H. T. Wang, H. M. Zhao, X. Quan, and S. Chen, "Electrochemical determination of tetracycline using molecularly imprinted polymer modified carbon nanotube-gold nanoparticles electrode," *Electroanalysis*, vol. 23, no. 8, pp. 1863–1869, 2011.